Simulation of Solids Processes Accounting for Particle-Size Distribution

Priscilla J. Hill and Ka M. Ng
Dept. of Chemical Engineering, University of Massachusetts, Amherst, MA 01003

A prototype computer program SOLIDS has been developed for the simulation of processes with solids processing steps. In addition to heat and mass balances, the equipment units are modeled with discretized population balance equations. Any transformation mechanisms for the particle-size distribution (PSD)—nucleation, growth, dissolution, agglomeration, and breakage—can be represented. With the sequential modular code, the PSD can be tracked from unit to unit in a complete plant. To provide maximum flexibility for further development, new or improved equipment models and discretization techniques can be included as additional subroutines. Case studies show that accounting for the PSD can lead to improved equipment design and a more complete description of the interactions among the units in the plant.

Introduction

Solids processing, which involves unit operations such as crushing, crystallization, dissolution, filtration, and drying, is prevalent throughout the chemical processing industries (CPI). Examples include the manufacture of salts, fertilizers, insecticides, herbicides, detergents, pigments, petrochemicals, and pharmaceuticals. According to recent estimates (Ennis et al., 1994; Nelson et al., 1995), 60% by value or volume of DuPont's products are sold in solid form and an additional 18% use particles as additives. Furthermore, at least 40% of the value added by the CPI is related to particle technology. Despite its major economic impact, technologies for solids processing are not as well developed as those for vapor and liquid processes. Extensive pilot-plant testing is often needed in the development of solids processes. Yet a study by Merrow (1985) shows that our performance in designing solids plants is still poor. In this survey of 37 solids plants, the average plant operated at 64% of its design capacity. When compared to vapor and liquid processes, which often operate at or above their design capacity, it is clear that there is need for improvement.

The incorporation of the properties and effects unique to solids in process design is critical in such an effort. For example, the particle-size distribution (PSD) plays a significant role in designing a hydrocyclone and a crystallizer. Filterability of a slurry depends on the particle shape, average size, and PSD; generally, a wider PSD leads to a lower filter cake porosity and permeability. Particle agglomeration depends on surface properties such as the zeta potential. Particle strength determines whether breakage occurs somewhere along the processing train. Processing units, which are of minor significance in modeling vapor–liquid processes, can become critical in solids processes. For example, control valves and pumps can produce excessive solids breakage and strongly influence the operations of the subsequent units. In addition to its effect on processing, product quality can also be affected by PSD. For example, the hiding power of pigments depends on the particle sizes relative to the wavelength of light (Depew and Eide, 1940; Allen, 1967). Also, solids can exhibit complex behavior such as the formation of enantiomers and polymorphs. Enantiopure drugs are now a $35 billion worldwide business (Stinson, 1994).

As a step toward the final goal of accounting for all these solids attributes in process design, the objective of this study is to formulate and demonstrate a systematic framework for the simulation of solids plants in which the PSD is included. Although most previous design studies are based on an average particle size, the need to follow the evolution of the PSD through the entire plant has been pointed out by a number of researchers (Neville and Seider, 1980; Jones, 1984; Barton and Perkins, 1988; Evans, 1989; Rajagopal et al., 1988, 1992; Hounslow and Wynn, 1992; Hill and Ng, 1995). This study has three major components:

- Develop a framework for the description of changes in the PSD from unit to unit in a complete plant. The numerical implementation of the formulation should be relatively easy. It should guarantee the correct prediction of changes in mass

Correspondence concerning this article should be addressed to K. M. Ng.

and total number of particles. This is achieved by using discretized population balance equations (PBEs) (Hill and Ng, 1995).

- Collect and/or formulate various solids processing models that reflect the impact of the PSD on the performance of the unit under consideration. This is necessary because many solids processing models are based on particles of an average size. As long as each unit operation model is consistent with the framework, it is a straightforward procedure to link the models together to simulate the entire system. In addition to the PBEs, mass and energy balances are used for the models.
- Develop a sequential modular simulation code to demonstrate the concepts. The effects of PSD and other unit operation design variables on the entire process are studied.

Framework for PSD Transformations

Transformation mechanisms

As a stream flows through an equipment unit, the PSD is altered by one or more mechanisms, depending on the equipment unit and the material being processed. These PSD transformations occur due to *variable-size* or *fixed-size* processes. In variable-size processes, changes in the PSD are due to chemical and physical changes to the size of individual particles. Typical mechanisms include particle agglomeration, breakage, dissolution, growth, and nucleation. Fixed-size processes refer to those in which the particles themselves remain intact as the PSD changes. One such process is mixing where two or more streams are combined into one stream. The other is mechanical separation, in which one stream is split into two or more streams. Mixing occurs in blenders and mixers. Mechanical separation takes place in hydrocyclones, screens, and filters.

Discretized population balance equations for variable-size processes

The use of population balance equations (PBEs) is essential in quantifying the variable-size transformations. A general form of the PBE is given below:

$$\frac{d}{dt}n(z,t;v) = [\text{Accumulation}] = [\text{Inflow}] - [\text{Outflow}] + [\text{Birth}] - [\text{Death}]. \quad (1)$$

Here, the dependent variable, $n(z,t;v)dv$, is the number concentration of particles between volumes v and $v + dv$ at position z and time t. The inflow (outflow) term accounts for the addition (removal) of particles to (from) the system. The birth term represents an increase in the number of particles due to nucleation, growth, dissolution, agglomeration, and/or breakage. Similarly, the death term represents a reduction in the number of particles due to growth, dissolution, agglomeration and/or breakage.

Solution of Eq. 1 is not straightforward. Analytical solutions exist but for a few idealized models. For realistic problems, a wide variety of methods for solving PBEs have been developed (Table 1). Most are numerical methods to directly solve the continuous PBE, while others are based on discretization of the continuous PBE with respect to particle size. That is, instead of the continuous variable $n(z,t;v)$, the discretized variable N_i, the number of particles in size interval i, is used. For reasons to be discussed below, the latter approach is chosen for process simulations.

Table 1. Methods of Solution for PBEs

Method of moments	(Hulburt and Katz, 1964)
Transform techniques	(Ramabhadran et al., 1976)
Method of weighted residuals	(Ramkrishna, 1971)
Approximation techniques	(Cohen and Vaughan, 1971)
Similarity solutions	(Ramabhadran and Seinfeld, 1975)
Monte Carlo simulation	(Shah et al., 1977)
Sectional representations	(Gelbard et al., 1980)
Discretization	(Hounslow et al., 1988; Kumar and Ramkrishna, 1996a,b)
Statistical analysis	(Davis, 1989)
Analytical solutions (primarily for breakage)	(Ziff, 1992)
Use of Fibonacci sequences	(Calabrese et al., 1992)
Use of probability functions	(Hill and Ng, 1995, 1996a)

Let us explain by casting Eq. 1 into a different form for a batch process. The discussions, however, are equally valid for a system with inflow and outflow.

$$\frac{d}{dt}n(z,t;v) = \left[\frac{d}{dt}n(z,t;v)\right]_{\text{Nucleation}} + \left[\frac{d}{dt}n(z,t;v)\right]_{\text{Growth}} + \left[\frac{d}{dt}n(z,t;v)\right]_{\text{Dissolution}} + \left[\frac{d}{dt}n(z,t;v)\right]_{\text{Agglomeration}} + \left[\frac{d}{dt}n(z,t;v)\right]_{\text{Breakage}} \quad (2)$$

Equation 2 shows that the changes in $n(z,t;v)dv$ are broken down into the basic transformation mechanisms. A batch process PBE that models breakage only is referred to as the breakage equation. Similarly, we also have the nucleation, growth, agglomeration, and dissolution equations.

Hill and Ng (1995) have developed the following discretized breakage equation:

$$\frac{d}{dt}N_i = \sum_{j=i+1}^{\infty} \beta_j b_{i,j} S_j N_j - \delta_i S_i N_i, \quad (3)$$

where $b_{i,j}$ is the number-based breakage distribution function, and S_i is the number-based specific rate of breakage. Here, β_j and δ_i are the birth term and death term correction factors. These two factors correct for the discretization error so that mass is conserved and the total number of particles is correctly predicted. Analytical expressions for these factors for a number of functional forms of $b_{i,j}$ are available. It should be mentioned that many breakage equations are on a mass basis; that is, instead of N_i, the dependent variable is the mass of particles within a given size range (Austin, 1976).

Similar discretized agglomeration equations exist. Some can correctly predict a single property such as the total number of particles or the total particle mass (Gelbard and Seinfeld, 1980; Sastry and Gaschignard, 1981). Others can correctly predict two properties such as the total number and volume of particles simultaneously (Hounslow et al., 1988; Hounslow, 1990; Litster et al., 1995; Hill and Ng, 1996a; Kumar and Ramkrishna, 1996a,b). In particular, Hill and Ng (1996a) have developed a discretized agglomeration equation for a PSD

with equal-size intervals or intervals with any geometric ratio larger than unity. For example, for a geometric ratio ≥ 2, the equation is

$$\frac{dN_i}{dt} = N_{i-1}\sum_{j=1}^{i-2} a_{i-1,j}N_j\left(\frac{\bar{v}_j}{\bar{v}_i-\bar{v}_{i-1}}\right) + N_i\sum_{j=1}^{i-1} a_{i,j}N_j\left(\frac{\bar{v}_{i+1}-\bar{v}_i-\bar{v}_j}{\bar{v}_{i+1}-\bar{v}_i}\right) + \frac{1}{2}a_{i-1,i-1}N_{i-1}^2\left(\frac{\bar{v}_{i-1}}{\bar{v}_i-\bar{v}_{i-1}}\right) + \frac{1}{2}a_{i,i}N_i^2\left(\frac{\bar{v}_{i+1}-2\bar{v}_i}{\bar{v}_{i+1}-\bar{v}_i}\right) - N_i\sum_{j=1}^{\infty} a_{i,j}N_j, \quad (4)$$

where $a_{i,j}$ is the agglomeration kernel, v_i is the largest particle size in interval i, and $\bar{v}_i$ is a representative particle size in interval i.

Similar equations are used for dissolution, growth, and nucleation (Hill, 1996). These equations have the following attributes:

- They provide an output discretized PSD that is guaranteed to have the same or nearly the same total number of particles and total mass of particles as that obtained from an exact solution of the fundamentally exact continuous PBE, Eq. 1.
- These discretized equations are flexible in that the user may choose equal-size intervals, where $v_i = iv_1$; or geometric-size intervals, where $v_i = r^{(i-1)}v_1$, for any value of r greater than or equal to 1. Using geometric-size intervals allows one to cover a wide range of particle sizes with a few size intervals.
- Discretized equations such as Eqs. 3 and 4 are ordinary differential equations that can be integrated in a routine manner.
- This approach is flexible. Since each transformation is described by ordinary differential equations, different equipment units can be modeled by combining the basic operations—agglomeration, breakage, dissolution, growth, and nucleation—that are appropriate for that equipment unit. For example, a crystallizer can use the terms for nucleation, growth, agglomeration, and breakage. Since a crusher may only involve breakage of particles, the breakage equation is used and the terms for other transformation mechanisms are set to zero.
- These equations fit in much better with the data structure used in large-scale simulation codes. With the exception of the standard continuous distributions such as the Gaussian, Rosin–Rammler, and log normal, it is easier to store an arbitrary PSD in discretized form in the computer program.

Transformation equations for fixed-size processes

Since the individual particles do not change in size for fixed-size processes, the total number of particles of size i is conserved. For example, when mixing streams 1 and 2 to form stream 3, we have

$$N_i(3) = \frac{q_1N_i(1) + q_2N_i(2)}{q_3}, \quad (5)$$

where $N_i(j)$ indicates the number of particles of size i per unit volume of slurry in stream j, and q_i is the volumetric flow rate for stream i. Note that $q_1 + q_2 = q_3$ may not be valid for mixing. When the streams have different compositions, volume is not conserved.

For the case where a stream is split into different streams, all of the streams have the same density. Therefore, if stream 1 is split to form streams 2 and 3, we have

$$q_1 = q_2 + q_3 \quad (6)$$

and

$$q_1N_i(1) = q_2N_i(2) + q_3N_i(3). \quad (7)$$

In addition, indication of how much material goes into each new stream is needed. For the hydrocyclone, the underflow to throughput ratio, R_{ut}, is a design variable where

$$R_{ut} = \frac{q_u}{q_f} \quad (8)$$

and where u and f indicate the underflow and feed streams, respectively. To determine the split of the particles, a grade efficiency curve, G_i, is used. That is,

$$N_i(u) = \frac{q_f}{q_u}N_i(f)G_i. \quad (9)$$

Empirical and theoretical expressions for G_i are available.

Equipment Models with Particle-Size Distribution

Solids processing equipment is notoriously difficult to model. One can formulate a complex model that considers all the underlying physics. However, such a model is usually very susceptible to numerical problems and is not suitable for large-scale process simulations. For robustness, one can formulate a simple model that often ends up as no more than a separation block. Efforts have been made to improve the solids processing models in some commercial simulation codes such as PRO/II and AspenPlus (Goldfarb et al., 1990). The aim is to strike a delicate balance between the desire to capture the PSD and as many critical equipment design variables as possible, and the robustness of the model in numerical simulation. This is illustrated with two examples.

Dissolvers

In this dissolver model, the liquid phase is assumed to be well mixed and the solid phase is in plug flow. Thus, dispersion is not considered for reasons of simplicity in process simulations. The dissolver volume, V_D, can be determined by

$$V_D = q\tau_D, \quad (10)$$

where τ_D is the residence time and q is the volumetric flow rate of the slurry. The dissolution rate depends on whether there is a chemical reaction.

Without a chemical reaction, the rate of dissolution is controlled by mass transfer as the system moves toward thermo-

dynamic equilibrium. The rate of dissolution of a spherical particle of component A of diameter D in a dissolver of temperature T_d is

$$-\frac{dD}{dt}=2k_C(D)\frac{\rho_{\text{solvent}}}{\rho_A}[S_A(T_d)-C_A]. \tag{11}$$

Here, k_C is the mass-transfer coefficient, ρ_{solvent} is the solvent density, ρ_A is the density of solid A, S_A is the solubility, and C_A is the concentration. The residence time it takes for the largest particle of diameter $D_{\max}$ to dissolve is

$$\tau=\int_0^{D_{\max}}\frac{\rho_A}{2k_C(D)\rho_{\text{solvent}}[S_A(T_d)-C_A]}dD. \tag{12}$$

When there is a chemical reaction, the rate of dissolution can be surface-reaction controlled, mass-transfer controlled, or in a mixed regime between surface-reaction and mass-transfer controlled (LeBlanc and Fogler, 1987, 1989). For a first-order reaction, the surface-reaction-controlled rate of dissolution is

$$-\frac{dD}{dt}=\frac{2kC}{\rho_A}, \tag{13}$$

where k is the rate of reaction constant, and C is the concentration of the reactant in the solution. When mass transfer is controlling, the rate is

$$-\frac{dD}{dt}=\frac{2Ck_c(D)}{\rho_A}. \tag{14}$$

For a first-order reaction, the mixed-regime dissolution rate is as follows:

$$-\frac{dD}{dt}=\frac{2kC}{\rho_A}\left[1+\frac{k}{k_c(D)}\right]^{-1}. \tag{15}$$

The residence time for the mixed regime is

$$\tau=\int_0^{D_{\max}}\frac{\rho_A}{2kC}\left[1+\frac{k}{k_c(D)}\right]dD. \tag{16}$$

For surface-reaction- or mass-transfer-controlled dissolution, Eq. 16 can be simplified by letting k_c or k go to infinity, respectively.

One has to account for the possibility that the user of the code has more solids than the given amount of solvent can dissolve. In that event, iteration is required to determine the PSD of the undissolved solids in the effluent of the dissolver. The dissolution rate depends on the outlet concentration; C_A in Eq. 12 and C in Eq. 16. These concentrations depend on the mass of solids dissolved, and the mass of solids dissolved in turn depends on the dissolution rate. Also, note that since the mass-transfer coefficient is a function of particle size, the dissolution rate changes with particle size as well.

Rotary vacuum filters

The filter area, A_F, depends on several parameters such as the filtrate viscosity, μ; the mass of solids per unit volume of filtrate in the slurry, χ; the permeability, k; the cake porosity, ϵ; the rotational speed, ω; the submergence, ψ; the volumetric flow rate of filtrate, q_f; and the pressure drop across the filter, Δp.

$$A_F=2\pi LR=\frac{2\pi q_f}{\omega}\left(\frac{2\rho_A(1-\epsilon)k\Delta p\psi}{\chi\mu\omega}\right)^{-1/2}. \tag{17}$$

Two of these parameters, permeability and cake porosity, are strongly influenced by the PSD. Permeability can be determined from the generalized Blake–Kozeny equation (MacDonald et al., 1991):

$$k=\frac{1}{180}\frac{\epsilon^3}{(1-\epsilon)^2}\left(\frac{m_2}{m_1}\right)^2, \tag{18}$$

where m_2 and m_1 are the second and first moments of the PSD with respect to particle diameter, respectively. The dependence of cake porosity on the PSD can be estimated by (Ouchiyama and Tanaka, 1984):

$$\epsilon=1-\frac{\sum_{i=1}^{m}D_i^3f_i}{\sum_{i=1}^{m}(D_i-\langle D\rangle)^3H(D_i-\langle D\rangle)f_i+\frac{1}{\bar{n}}\sum_{i=1}^{m}\left\{(D_i+\langle D\rangle)^3-(D_i-\langle D\rangle)^3H(D_i-\langle D\rangle)\right\}f_i}, \tag{19}$$

where

$$\bar{n}=1+\frac{4(7-8\bar{\epsilon}_0)\langle D\rangle}{13}\frac{\sum_{i=1}^{m}(D_i+\langle D\rangle)^2\left(1-\frac{3}{8}\frac{\langle D\rangle}{D_i+\langle D\rangle}\right)f_i}{\sum_{i=1}^{m}\left\{D_i^3-(D_i-\langle D\rangle)^3H(D_i-\langle D\rangle)\right\}f_i}, \tag{20}$$

where f_i is the number fraction of particles in interval i; $\bar{\epsilon}_0$ is the overall average porosity of uniformly sized spheres; H is the Heaviside function, and $\langle D \rangle$ is the mean particle diameter. The development of Eqs. 19 and 20 were based on data for a limited number of size intervals. Our simulations can include more than 20 intervals and a much wider range of particle sizes. We found that calculations with this model for so many size intervals produce unreasonably low porosities. For this reason, size intervals at the two ends of the PSD and with less than 5% of the total mass are truncated. However, all the size intervals are used to calculate the moment ratio in Eq. 18. In developing the computer code, we have kept the complexity of our models relatively low to minimize our simulation efforts. The filter model can be extended to include filter-medium resistance, as well as filter-cake washing and dewatering, if desirable, at a later stage.

Other equipment models

Equipment models such as hydrocyclones, crystallizers, and others as needed are also included in the program. Again, since discretized equations are used, the user is not limited to the special cases where solutions exist. For example, crystal breakage is ignored in many of the crystallizer models in the literature (Marchal et al., 1988; Hounslow, 1990; Saleeby and Lee, 1994; Lee and Saleeby, 1994). Since expressions for all of the mechanisms have the same basis, these mechanisms are easily combined as in Eq. 2. Here, we model a mixed-suspension–mixed-product-removal (MSMPR) crystallizer by assuming that both the liquid and the solid phases are well mixed. This model is flexible in that it includes all of the mechanisms listed before and it can perform the calculations with or without seeds in the feed stream.

Model Parameters with Particle-Size Distribution

In addition to the trade-off between the completeness of the model and potential numerical problems, another important consideration is the availability of model parameter values. For example, plug flow is assumed for the solids phase in the dissolver model primarily because we lack the dispersion coefficients for suspended particles in stirred tanks. Another issue is the reliability of the model parameters. While the permeability and porosity predictions can offer reasonable values in the absence of experimental data, as can be seen in the discussion on Eqs. 19 and 20, it is important to note the range of applicability of these predictions. For crystallization, Farrell and Tsai (1994) discussed the importance and difficulty of accurately determining kinetic parameters for various process conditions. Hill and Ng (1996b) showed that empirical data for multiple particle breakage can be represented by various breakage function parameters. Also, emphasis should be placed on model parameters that are common to related equipment units. This is illustrated below for breakage.

Breakage in pipes and vessels

In simulating a steady-state gas–liquid process, pipes, pumps, and valves are often not modeled because no material changes take place in these units. However, as in crushers, grinders, and crystallizers, particle breakage can occur. Thus, pipes, pumps, and vessels can share the same breakage model parameters, while having other parameters specific to an individual equipment item.

Table 2. Breakage Parameters for Process Equipment

Equipment Unit	Breakage Parameters	Reference
Crusher	$b_{i,j}$, S_i	Austin et al. (1976)
Pipeline	$b_{i,j}$, S_i, $\dot{\gamma}$	Karabelas (1976)
Pumps	$b_{i,j}$, S_i	Shook et al. (1978)
	$\dot{\gamma}$	Hoare et al. (1982)
Stirred Tank	L, M_T, $\bar{\epsilon}$	Conti and Nienow (1980); Nienow and Conti (1978)
	$B_{i,j}$	Mazzarotta (1992)
	L^5, $\bar{\epsilon}$	Synowiec et al. (1993)

Table 2 summarizes the parameters used in various breakage models. Attrition is often quantified by $b_{i,j}$ and S_i, and these in turn depend on factors such as equipment geometry and the material being broken (Austin et al., 1976; Shook et al., 1978; Mazzarotta, 1992). Others have shown that other operating parameters are important. For example, Karabelas (1976) showed that the particle attrition of coal slurries in pipelines depends on the shear rate, $\dot{\gamma}$. Another study with pumps (Hoare et al., 1982) shows a similar dependence on the shear rate. Studies on stirred tanks by Nienow and Conti (1978), and Conti and Nienow (1980) show that the rate of breakage depends on the parent particle size, L. In a recent paper by Synowiec et al. (1993) on agitated suspensions of potassium sulfate and potash alum crystals, the change in PSD is a function of the parent particle size and the specific power input, $\bar{\epsilon}$.

Complete Plant Simulations

The general framework as well as various solids processing models have been implemented in a sequential modular code SOLIDS written in FORTRAN for steady-state process simulations. The main program of SOLIDS accepts various parameter values and initial condition data. It then calls a subroutine for each equipment unit in the process and provides connections between the process units. Each process unit subroutine can call other subroutines as needed. For example, the subroutine MSMPR performs calculations related to stoichiometry and component concentrations in the crystallizer mother liquor, and it calls other subroutines to solve the PBEs. The main program also determines when the simulation has converged. For systems with recycle streams, the same rules for vapor–liquid processes apply. For example, if there are two recycle loops with one common stream, then it should be the tear stream. Iterations begin with estimated values of the component concentrations, flow rate, and PSD for the selected tear stream in the recycle loop. Convergence is obtained when the changes of these quantities fall within the specified tolerances with successive iterations. Three simplified case studies are presented below to illustrate the effect of PSD as well as other design variables on solids processes.

Potash production

Potash is often produced from sylvinite, a mixture of KCl and NaCl, by using dissolution, crystallization, and filtration.

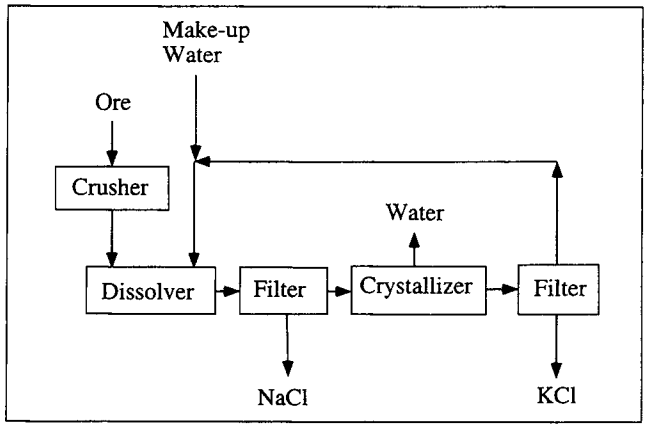

Figure 1. Flowsheet for potash production from sylvinite ore.

A simplified flow sheet is presented in Figure 1. The ore is crushed before it is mixed with water and heated to a relatively high temperature in the dissolver. Because of the effect of temperature on the joint solubility, all of the KCl is dissolved while most of the NaCl remains as a solid. The solid NaCl is removed from the slurry in the first filter and the KCl-rich liquid is fed to the crystallizer. By cooling the solution to a lower temperature and evaporating water in the crystallizer, KCl crystallizes, and NaCl is left in solution. The KCl crystals are removed in the second filter and the mother liquor is recycled to the dissolver. The only NaCl that leaves with the product is in the residual liquid. Water is added to the mother-liquor recycle stream to make up for the amounts lost through evaporation and trapped in the filter cakes. Thus, the total amount of water flowing into the dissolver, W, is the sum of the makeup water and the water recycled from the second filter. The input parameters used for this case study are summarized in Table 3.

Rajagopal et al. (1988) studied the same process using the dominant crystal size. To show the possible error caused by ignoring the PSD, simulations are performed with the mean particle size $\langle D \rangle$ and with the PSD. Figure 2 shows such effects on the dissolver residence time, τ_D, as a function of the total amount of water flowing into the dissolver. As W is increased, the solution in the dissolver becomes more dilute and there is a larger driving force for dissolution. With the increased driving force, the rate of dissolution increases, the

Table 3. Selected Input for the Potash Plant

Sylvinite ore composition	
KCl	40 wt. %
NaCl	60 wt. %
Feed-flow rates	
Ore	1,859 kg/min
Densities	
KCl	2,000 kg/m^3
NaCl	2,160 kg/m^3
Crystallizer	
Operating temperature	30°C
Agglomeration kernel	0 (no./m^3)$^{-1}$/min
Breakage rate	0 min^{-1}
Growth rate	4.2 μm/min
Nucleation rate	$6.57\times10^5\ M_T^{0.14}\ G^{4.99}$ no./min/m^3
Dissolver	
Operating temperature	100°C
Mass-transfer coefficient, k_c	1,206 μm/min
Filter	
Rotation speed, ω	10 rpm
Vacuum level, Δp	35,000 N/m^2
Angle of submergence, ψ	145°
Filtrate viscosity, μ	1.00 cp at 20°C 0.28 cp at 100°C
Residual liquid saturation after dewatering in the filter cake	0.155
Filter-cake porosity, $\bar{\epsilon}_0$	0.412
Crusher	
Grinding time	1 min

Using the equation by Austin et al. (1976):

$$B_M(v,w) = \phi\left(\frac{v}{w}\right)^{\gamma/3} + (1-\phi)\left(\frac{v}{w}\right)^{\beta'/3}, \qquad (21)$$

$S_c = 1.5/10^4$ min^{-1}	$\alpha = 0.34667$
$\beta' = 4.0$	$\phi = 0.36$
$\gamma = 1.17$	$\sigma = 20.0\ \mu$m^3

where S_c is the breakage rate constant, α is the breakage-rate power-law exponent, and σ is the smallest possible particle size (Hill and Ng, 1995).

Source: Rajagopal et al., 1988.

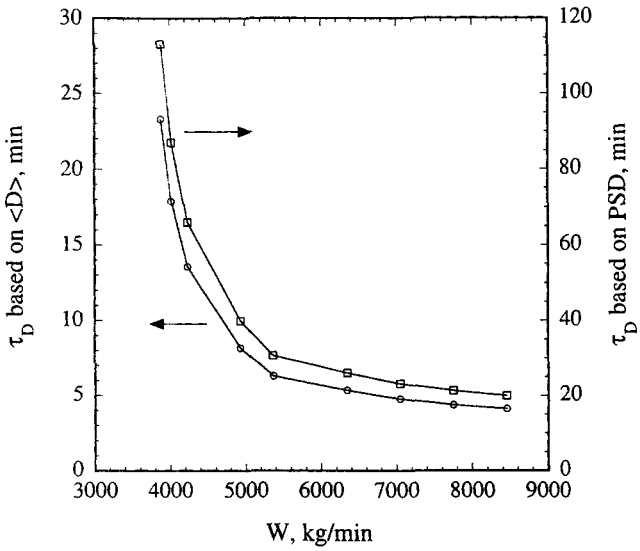

Figure 2. Dissolver residence time as a function of the total water flow rate.

dissolution proceeds more quickly, and therefore, the residence time shortens. For all values of W, using $\langle D \rangle$ underpredicts the residence time by a factor of around 4 to 5. The reason for the discrepancy is simply that the residence time is dictated by the time required to completely dissolve the largest particle in the population. The use of the mean particle size for design underestimates the necessary dissolver volume and can lead to incomplete dissolution of the larger particles.

The PSD also has a strong effect on filter area. Figure 3 shows the dissolver filter area as a function of the total water flow rate into the dissolver using both $\langle D \rangle$ and the PSD. With the mass-flow rate of solids fixed, the filter area increases with filtrate throughput for both sets of calculations. The slightly nonlinear dependence on the flow rate is due to the square-root factor in Eq. 17. The filter area calculated using the mean particle size is smaller than that calculated

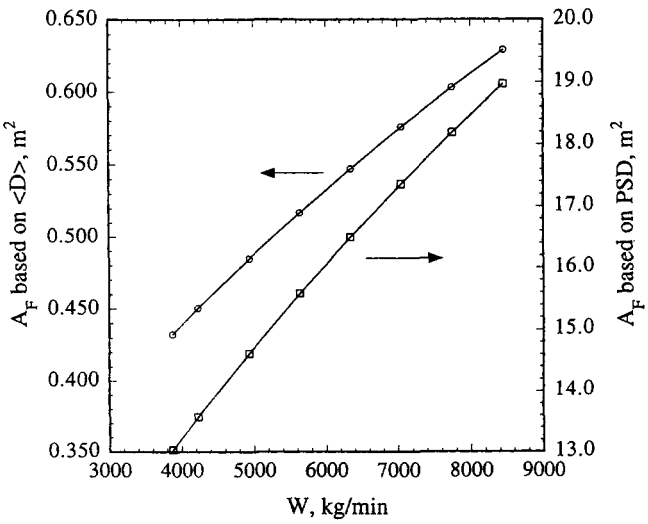

Figure 3. Filter area of the filter after the dissolver as a function of the total water flow rate.

using the PSD by two orders of magnitude for two reasons. First, a ratio of moments, m_2/m_1, is used as the characteristic length to determine the permeability, k, in the PSD calculations (Eq. 18). The mean particle size $\langle D \rangle$ is an order of magnitude larger than m_2/m_1 and this leads to a larger permeability and a smaller filter area. Second, the porosity model (Eqs. 19 and 20) predicts a porosity of 0.35 from the PSD. However, a porosity of 0.40 is assumed for the mean particle-size calculations. This larger porosity again leads to a smaller filter area.

Salt production

Figure 4 shows a flow sheet for the production of salt by mining a salt dome (Hester and Diamond, 1955; Rossiter and Douglas, 1986a,b). In this process, the brine from the mine is pumped into an evaporative crystallizer, where salt crystals are formed as the water is removed by evaporation. The production rate P is fixed. The resulting slurry of salt crystals and brine is sent to a hydrocyclone. The overflow is recycled and αP is the mass flow rate of solids in the overflow. The underflow is sent to a filter where the mother liquor is removed and recycled to the crystallizer, and the salt is recovered as a filter cake. We assume that the brine from the mine and the recycle stream from the filter do not have any solid particles. Impurities such as calcium sulfate, calcium chloride, and magnesium chloride are not considered. The operating conditions for the base-case simulation are shown in Table 4. We have chosen to study the effects of each of the design variables α, R_{ut}, and M_T on the process. Here, the underflow-to-throughput ratio, R_{ut}, is the volumetric flow rate of slurry in the underflow to that in the feed. M_T is the magma density.

The mass of recycled solids has a strong effect on the crystallizer. Figure 5 shows the dependence of the volumetric flow rate of slurry, q_{out}, and the residence time, τ_C, on α. Since the mass-flow rate of solids exiting the crystallizer, M_{so}, is equal to $(1+\alpha)P$ and P is fixed, M_{so} increases as α is increased. Therefore, q_{out} also increases with α because q_{out} is equal to M_{so}/M_T, and M_T is a constant. The decrease in residence time with increasing α implies that the overall crystal growth rate is higher with recycled crystals.

The amounts of water and salt crystals recycled to the crystallizer remain the same when R_{ut} is changed. However, the filter area required increases as a function of R_{ut} (Figure 6). Increasing R_{ut} increases the amount of filtrate for the same

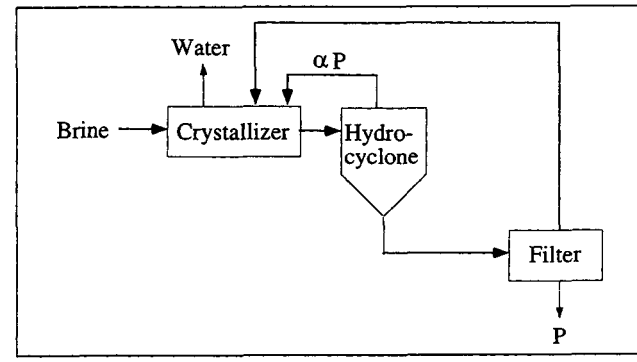

Figure 4. Flowsheet for salt production from brine.

Table 4. Selected Input Data for the Salt Plant

Production rate	10^5 ton/yr = 185.4 kg/min
Feed concentration	214.6 kg NaCl/m^3 solution
Liquid fraction in feed	$\epsilon_f = 1.0$
Solubility of NaCl	$S_N = 0.35712 + 8.48 \times 10^{-5}\, T + 3.17 \times 10^{-6}\, T^2$ kg NaCl/kg H_2O
Densities	
NaOH	2,163 kg/m^3
H_2O	1,000 kg/m^3
Crystallizer	(Garside and Shah, 1980)
Operating temperature	50°C
Agitator speed, N	500 rpm
Agglomeration kernel	0 (no./m^3)$^{-1}$/min
Breakage rate	0 min^{-1}
Growth rate	6 μm/min
Nucleation rate	0.32 $N^2\, G^2\, M_T$ no./min/m^3
M_T	105.8 kg/m^3
Hydrocyclone	
α	0.2
R_{ut}	0.15
Filter	
Rotation speed, ω	5 rpm
Angle of submergence, ψ	145°
Vacuum level, Δp	3,500 N/m^2
Filter-cake porosity, $\bar{\epsilon}_0$	0.412

production rate, P. Clearly, it is desirable to operate at the lowest underflow-to-throughput ratio from an economic standpoint.

The dependence of crystallizer volume, V_C, and the volumetric flow rate of the crystallizer effluent stream, q_{out}, on magma density is shown in Figure 7. As discussed previously with α fixed, M_{so} is also fixed. Clearly, q_{out} $(= M_{so}/M_T)$ decreases with increasing magma density, M_T. The decrease in crystallizer volume with increasing M_T implies that the overall crystal growth rate is higher with increasing magma density.

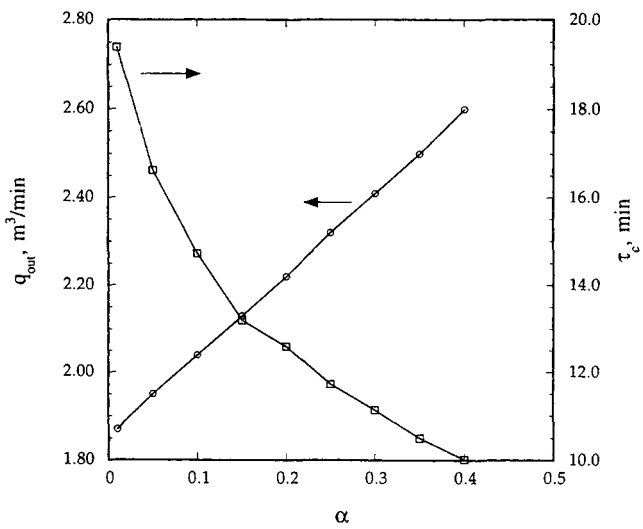

Figure 5. Volumetric flow rate of slurry exiting the crystallizer and crystallizer residence time vs. the quantity of recycled solids.

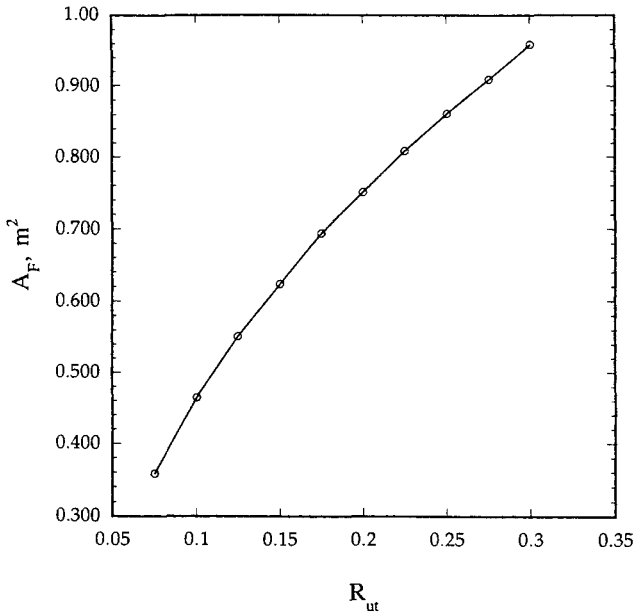

Figure 6. Filter area as a function of underflow-to-throughput ratio.

Bayer process

The Bayer process is used almost exclusively for the extraction of alumina from bauxite (Misra, 1986). A simplified flow sheet is shown in Figure 8. Initially, the bauxite ore is crushed to reduce the time required for extraction. A hot solution of concentrated sodium hydroxide (150 to 250°C) reacts with the aluminum hydroxide minerals in bauxite according to the following reaction:

$$Al_2O_3 \cdot 3H_2O_{(S)} + 2NaOH_{(l)} \leftrightarrow Al_2O_3 \cdot Na_2O_{(l)} + 4H_2O \quad (22)$$

to produce sodium aluminate, $NaAlO_2$. Various impurities,

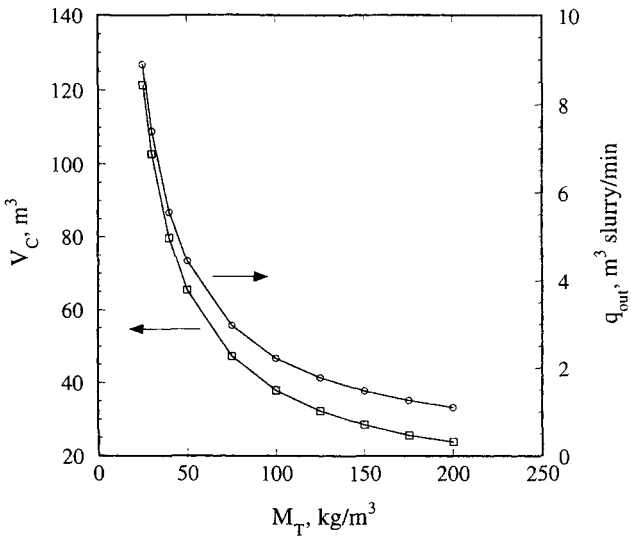

Figure 7. Crystallizer volume and volumetric flow rate of the crystallizer effluent stream as functions of magma density.

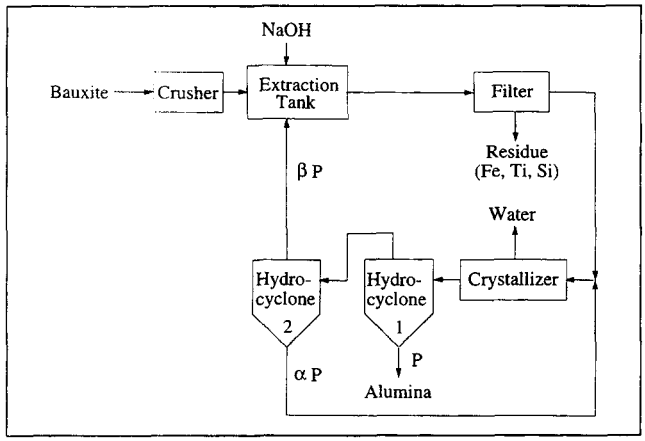

Figure 8. Flowsheet for the production of alumina by the Bayer process.

mainly oxides of iron, titanium, and silicon, are present in the feed. We assume that only ferric oxide is present and it reacts with sodium hydroxide in the following reaction:

$$Fe_2O_3{\cdot}3H_2O_{(S)} + 2NaOH_{(l)} \leftrightarrow Fe_2O_3{\cdot}Na_2O_{(l)} + 4H_2O. \quad (23)$$

Due to reaction equilibrium, there is a maximum concentration of $Fe_2O_3{\cdot}Na_2O$ in the extraction tank effluent. Some of the $Fe_2O_3{\cdot}3H_2O$ may not react and remains as a solid. The separation of insoluble from the caustic aluminate solution is done by filtration. The solid-free caustic aluminate solution is then cooled (60 to 70°C) and seeded to obtain crystalline aluminum trihydroxide ($Al(OH)_3$), which is recovered in the underflow of the first hydrocyclone. The washed trihydroxide is dehydrated by calcination to obtain alumina (Al_2O_3). Seeds are obtained from the underflow of the second hydrocyclone. The caustic liquor in the overflow is recycled back to the extraction step. The input data for the base case are given in Table 5.

Table 5. Selected Input Data for the Alumina Plant

Bauxite composition	
$Al_2O_3{\cdot}3H_2O$	60 wt. %
$Fe_2O_3{\cdot}3H_2O$	40 wt. %
Sodium hydroxide composition	
C_{NaOH}	770 kg NaOH/m^3 solution
Feed-flow rates	
Ore	484 kg/min
NaOH solution	0.2 m^3/min
Crystallizer data	
Agglomeration kernel	$1/10^{14}$ (no./m^3)$^{-1}$/min (Halfon and Kaliaguine, 1976)
Breakage rate	0 min^{-1}
Growth rate	1 μm/h (Misra and White, 1971)
Nucleation rate	1.66×10^{10} no./min/m^3 (Misra and White, 1971)
Dissolver	
Dissolution rate	0.752 (kg/m^{3}liq)$^{-1}\mu$m/min
Hydrocyclone	
$R_{ut,1}$	0.15
$R_{ut,2}$	0.15
Crusher	
Grinding time	30 min
Using Eq. 21:	
$S_c = 1.5/10^4$ min^{-1}	$\alpha = 0.34667$
$\beta' = 4.0$	$\phi = 0.36$
$\gamma = 1.17$	$\sigma = 20.0$

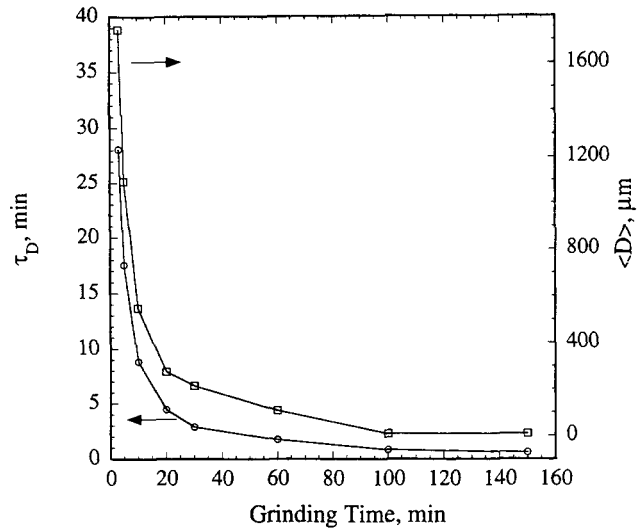

Figure 9. Dissolver residence time and mean particle diameter as functions of the grinding time.

Figure 9 shows the dissolver residence time, τ_D, and the mean particle diameter as functions of grinding time. Increasing the grinding time from 0 to 30 min greatly reduces the dissolver residence time, but grinding for longer than 30 min has little effect on τ_D. Since the dissolver volume is directly related to the residence time, the volume decreases as the particle size entering the dissolver decreases. However, as the particles are ground to smaller sizes, the grinding costs increase. An optimum grinding time depending on a trade-off between grinding and dissolution costs is expected.

The amount of grinding also impacts the filter downstream of the dissolver. Figure 10 shows the mean particle diameter,

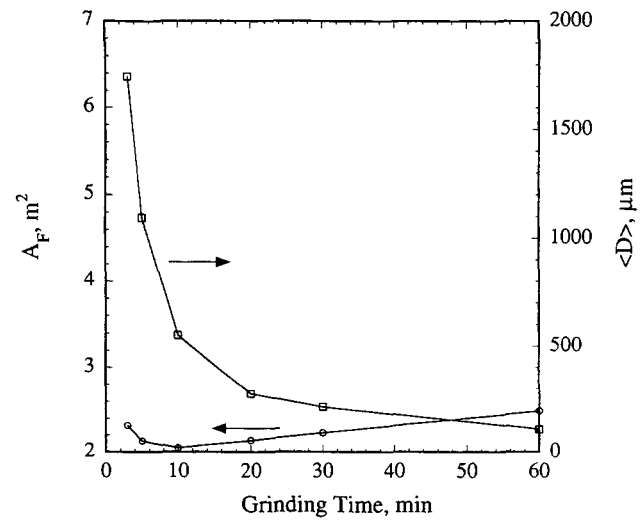

Figure 10. Filter area and mean particle diameter as functions of the grinding time.

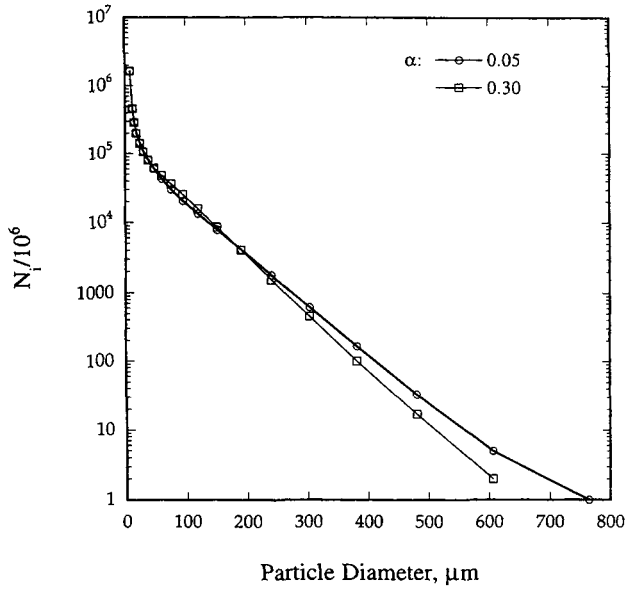

Figure 11. Particle-size distributions for $\alpha = 0.05$ and $\alpha = 0.30$.

$\langle D \rangle$, of the impurities as a function of grinding time. As expected, $\langle D \rangle$ decreases steadily with grinding time. The filter area, A_F, however, decreases for the first 10 minutes of grinding before increasing with grinding time. According to Eqs. 19 and 20, a small amount of grinding in the first 10 minutes actually causes a slight increase in porosity, thus causing the peculiarity observed in the simulations.

In this case study, α denotes the mass ratio of seeds recycled to the crystallizer to the solids produced and is expected to influence the crystallizer performance. Figure 11 shows that increasing α produces a PSD with fewer large particles, or a narrower distribution due to a combination of nucleation, growth, and agglomeration effects. The mass ratio of solids

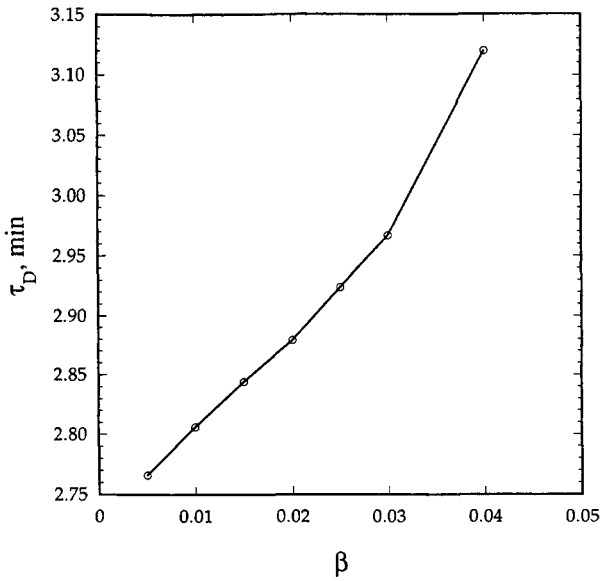

Figure 12. Dissolver residence time as a function of the fraction of solids recycled to the dissolver.

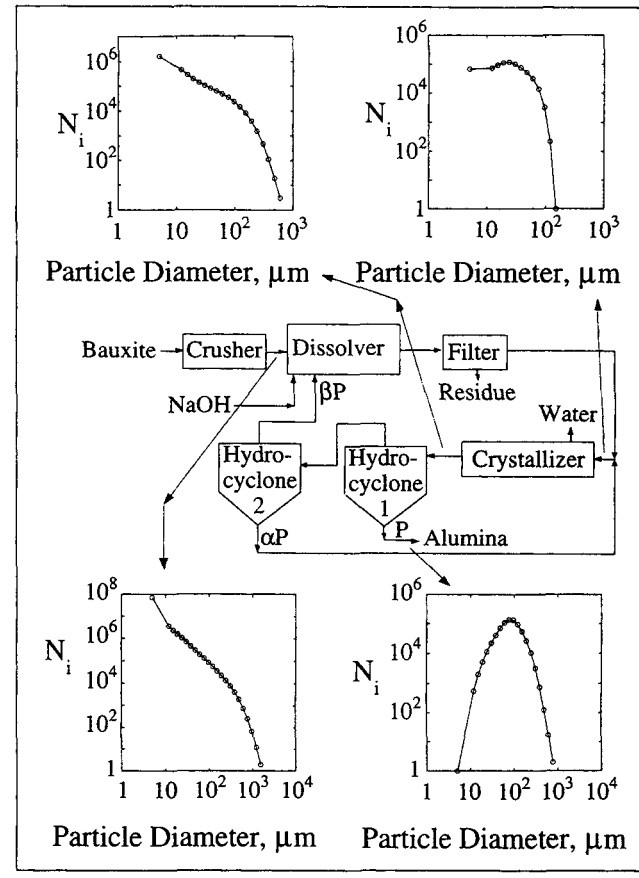

Figure 13. PSDs for various streams in the Bayer process.

recycled to the dissolver to solids produced, denoted by β, also influences the process, although it is usually small. Figure 12 shows that the dissolver residence time, τ_D, increases almost linearly as β is increased from 0.005 to 0.04. This is expected since there are more solids to dissolve.

In order to follow the evolution of the PSD in an entire process, it is helpful to view the PSD at several points in the process. Figure 13 shows the PSD of the streams entering and exiting the crystallizer as well as the stream entering the dissolver and the final product stream. Each case is plotted as a log-log plot with a minimum particle diameter of 1 μm. For the crystallizer, it is interesting to see how maximum particle size increases and how the number of small particles increases due to nucleation.

Conclusions

Because of the economic significance of solids processes, considerable research is taking place to improve the associated technologies. The progress is evident from the activities within the Particle Technology Forum of the American Institute of Chemical Engineers. Clearly, it is highly desirable to incorporate the current solids processing technologies into computer-aided process design and simulations (Bridgwater, 1995).

Toward this goal, this study is an attempt to include PSD in the process simulation of a complete plant. As mentioned, this problem was tackled by a number of researchers (Jones,

1984; Barton and Perkins, 1988) in the past. The major difference is that discretized PBEs have been chosen in our approach. The number density function is discretized into a number of size intervals. The integrodifferential equations are transformed into a set of ordinary differential equations. We developed our own discretization procedures because it is critical to have a comprehensive coherent set of techniques for the various transformation mechanisms. However, if desirable, other discretization techniques can be easily implemented in the code SOLIDS as additional subroutines.

Actually, discretized PSDs in a sense are used in PRO/II and Aspen Plus for a limited number of solids processing models in isolation. What we have demonstrated is that a wide variety of equipment units can be linked together for the entire plant using the same general framework of discretized population balance equations. Both the total mass and number of particles are predicted correctly as the PSD evolves from unit to unit in a complete plant. Despite the relatively large increase in the number of variables, convergence is not unduly difficult. Also, other process simulations involving probability density functions exist. Modeling of polymerization is now available in Polyred (Hyprotech) and Polymers Plus (Aspen Technology).

The familiar sequential modular approach is used to provide maximum flexibility. Other equipment or parameter models can be added to the code by the user. Depending on the PSD transformation mechanisms required, the discretization subroutines for those mechanisms can be called to form the proper set of ordinary differential equations. If experimental data such as filter-cake resistance are available for some of the process parameters, of course, the user can bypass those equations in the code and input the experimental values. An obvious extension is to convert SOLIDS to an equations-based simulation code so as to handle dynamic simulations.

Three case studies—the production of potash, salt, and alumina—are performed. The PSD is shown to play an important role in equipment sizing. This is demonstrated by performing two sets of calculations in which one set uses the mean particle size and the other accounts for the PSD. For both the dissolver and the subsequent filter in the potash process, the two sets of calculations yield significantly different results. Some design variables are unique to solids plants. It is shown in the salt plant that the way in which the hydrocyclone operates, as characterized by the amount of solids in the overflow and the underflow-to-throughput ratio, can impact both the upstream crystallizer volume and the downstream filter area. Another example of how the PSD influences an upstream unit is illustrated in the alumina process. The PSD of the product depends on the amount of seeds recycled from a downstream hydrocyclone to the crystallizer.

We have demonstrated with SOLIDS the feasibility and some of the advantages of accounting for the PSD in process simulations. Obviously, much more work is needed before it can be used to simulate commercial processes with complex flow-sheet structures, and with advanced solids processing equipment such as various granulators, classifiers, combined filter-dryers, metering devices, and so on. Actually, additional work is also needed for conventional equipment units. For example, it is well-known that attrition can be a significant problem in cyclones, yet we are not aware of the existence of a general, reliable model. The inclusion of other solids attributes such as shape, defects, and occlusions in simulations is also critical in realistic process evaluations. Better ways to estimate model parameters would help improve the accuracy of the predictions. However, as mentioned earlier, significant progress is being made in the fundamentals of particle technology. It is hoped that this study provides a platform for rapidly incorporating those advances into process design so as to achieve the highest economic potential for a plant from a systems perspective.

Acknowledgment

The support of the National Science Foundation (grant CTS-9211673) for this research is gratefully acknowledged.

Notation

a_{ij} = discretized form of coalescence kernel for interactions between intervals i and j for constant kernel (no. min)$^{-1}$, and linear kernel (no. μm^3·min)$^{-1}$
L = length of rotary vacuum filter, m
$n(v)$ = number density function, no./μm^3/m^3
N = agitation speed, rpm
P = solid-product flow rate, kg/min
R = radius of rotary vacuum filter, m
S_c = constant for the rate of breakage, μm$^{-3\alpha}$·min^{-1}
α = power-law exponent for specific rate of breakage, dimensionless
σ = limiting size of particle, volume basis, μm^3

Literature Cited

Allen, T., "Particle Size Measurements and Their Significance," *Pigments. An Introduction to Their Physical Chemistry*, D. Patterson, ed., Elsevier, New York (1967).

Austin, L., K. Shoji, V. Bhatia, V. Jindal, K. Savage, and R. Klimpel, "Some Results on the Description of Size Reduction as a Rate Process in Various Mills," *Ind. Eng. Chem. Process Des. Develop.*, **15**, 187 (1976).

Barton, G. W., and J. D. Perkins, "Experiences with SPEEDUP in the Mineral Processing Industries," *Chem. Eng. Res. Des.*, **66**, 408 (1988).

Bridgwater, J., "Particle Technology," *Chem. Eng. Sci.*, **50**, 4081 (1995).

Calabrese, R. V., M. H. Wang, N. Zhang, and J. W. Gentry, "Simulation and Analysis of Breakage Phenomena," *Trans. Ind. Chem. Eng.*, Part A, **70**, 189 (1992).

Cohen, E. R., and E. U. Vaughan, "Approximation Solution of the Equation for Aerosol Agglomeration," *J. Colloid Interface Sci.*, **35**, 612 (1971).

Conti, R., and A. W. Nienow, "Particle Abrasion at High Solids Concentration in Stirred Vessels—II," *Chem. Eng. Sci.*, **35**, 543 (1980).

Davis, H. T., "On the Statistics of Randomly Broken Objects," *Chem. Eng. Sci.*, **44**, 1799 (1989).

Depew, H. A., and A. C. Eide, "Effect of Particle Shape of White Pigments on Opacity," *Ind. Eng. Chem.*, **32**, 537 (1940).

Ennis, B. J., J. Green, and R. Davies, "Particle Technology: The Legacy of Neglect in the U.S.," *Chem. Eng. Prog.*, **90**(4), 32 (1994).

Evans, L. B., "Simulation with Respect to Solid Fluid Systems," *Comput. Chem. Eng.*, **13**, 343 (1989).

Farrell, R. J., and Y. C. Tsai, "Modeling, Simulation and Kinetic Parameter Estimation in Batch Crystallization Processes," *AIChE J.*, **40**, 586 (1994).

Garside, J., and M. B. Shah, "Crystallization Kinetics from MSMPR Crystallizers," *Ind. Eng. Chem. Process Des. Develop.*, **19**, 509 (1980).

Gelbard, F., and J. H. Seinfeld, "Simulation of Multicomponent Aerosol Dynamics," *J. Colloid Interface Sci.*, **78**, 485 (1980).

Gelbard, F., Y. Tambour, and J. H. Seinfeld, "Sectional Representations for Simulating Aerosol Dynamics," *J. Colloid Interface Sci.*, **76**, 541 (1980).

Goldfarb, S., J. Coon, J. Tanger, K. M. Ng, and C. F. Chu, "Crystallization Process Optimization Using PRO/II," AIChE Meeting, Chicago (1990).
Halfon, A., and S. Kaliaguine, "Alumina Trihydrate Crystallization, Part 2. A Model of Agglomeration," *Can. J. Chem. Eng.*, **54**, 168 (1976).
Hester, A. S., and H. W. Diamond, "Salt Manufacture," *Ind. Eng. Chem.*, **47**, 672 (1955).
Hill, P. J., *Simulation of Solids Processes Accounting for Particle Size Distribution*, PhD Thesis, University of Massachusetts, Amherst (1996).
Hill, P. J., and K. M. Ng, "New Discretization Procedure for the Breakage Equation," *AIChE J.*, **41**, 1204 (1995).
Hill, P. J., and K. M. Ng, "A New Discretization Procedure for the Agglomeration Equation," *AIChE J.*, **42**, 727 (1996a).
Hill, P. J., and K. M. Ng, "Statistics of Multiple-Particle Breakage," *AIChE J.*, **42**, 1600 (1996b).
Hoare, M., T. J. Narendranathan, J. R. Flint, D. Heywood-Waddington, D. J. Bell, and P. Dunnill, "Disruption of Protein Precipitates during Shear in Couette Flow and in Pumps," *Ind. Eng. Chem. Fundam.*, **21**, 402 (1982).
Hounslow, M. J., "A Discretized Population Balance for Continuous Systems at Steady State," *AIChE J.*, **36**, 106 (1990).
Hounslow, M. J., R. L. Ryall, and V. R. Marshall, "A Discretized Population Balance for Nucleation, Growth and Aggregation," *AIChE J.*, **34**, 1821 (1988).
Hounslow, M. J., and E. J. W. Wynn, "Modelling Particulate Processes: Full Solutions and Short Cuts," *Comput. Chem. Eng.*, **16**(Suppl.), S411 (1992).
Hulburt, H. M., and S. Katz, "Some Problems in Particle Technology. A Statistical Mechanical Formulation," *Chem. Eng. Sci.*, **19**, 555 (1964).
Jones, G. L., "Simulating the Effects of Changing Particle Characteristics in Solids Processing," *Comput. Chem. Eng.*, **8**, 329 (1984).
Karabelas, A. J., "Particle Attrition in Shear Flow of Concentrated Slurries," *AIChE J.*, **22**, 765 (1976).
Kumar, S., and D. Ramkrishna, "On the Solution of Population Balance Equations by Discretization—I. A Fixed Pivot Technique," *Chem. Eng. Sci.*, **51**, 1311 (1996a).
Kumar, S., and D. Ramkrishna, "On the Solution of Population Balance Equations by Discretization—II. A Moving Pivot Technique," *Chem. Eng. Sci.*, **51**, 1333 (1996b).
LeBlanc, S. E., and H. S. Fogler, "Population Balance Modeling of the Dissolution of Polydisperse Solids: Rate Limiting Regimes," *AIChE J.*, **33**, 54 (1987).
LeBlanc, S. E., and H. S. Fogler, "Dissolution of Powdered Minerals: The Effect of Polydispersity," *AIChE J.*, **35**, 865 (1989).
Lee, H. W., and E. G. Saleeby, "Mathematical Behavior of the Population Balance of a MSMPRC with Agglomeration, Feed and Size-Dependent Growth Rate," *Comput. Chem. Eng.*, **18**, 899 (1994).
Litster, J. D., D. J. Smit, and M. J. Hounslow, "Adjustable Discretized Population Balance for Growth and Aggregation," *AIChE J.*, **41**, 591 (1995).
MacDonald, M. J., C. F. Chu, P. P. Guilloit, and K. M. Ng, "A Generalized Blake-Kozeny Equation for Multisized Spherical Particles," *AIChE J.*, **37**, 1583 (1991).
Marchal, P., R. David, J. P. Klein, and J. Villermaux, "Crystallization and Precipitation Engineering—I. An Efficient Method for Solving Population Balance in Crystallization with Agglomeration," *Chem. Eng. Sci.*, **43**, 59 (1988).
Mazzarotta, B., "Abrasion and Breakage Phenomena in Agitated Crystal Suspensions," *Chem. Eng. Sci.*, **47**, 3105 (1992).
Merrow, E. W., "Linking R&D to Problems Experienced in Solids Processing," *Chem. Eng. Prog.*, **81**(5), 14 (1985).
Misra, C., *Industrial Alumina Chemicals*, ACS Monograph 184, American Chemical Society, Washington, DC (1986).
Misra, C., and E. T. White, "Kinetics of Crystallization of Aluminum Trihydroxide from Seeded Caustic Aluminate Solutions," *Crystallization from Solution: Factors Influencing Size Distribution*, M. A. Larson, ed., AIChE Symp. Ser., **67**, 53 (1971).
Nelson, R. D., R. Davies, and K. Jacob, "Teach 'Em Particle Technology," *Chem. Eng. Educ.*, **29**, 12 (1995).
Neville, J. M., and W. D. Seider, "Coal Pretreatment—Extensions of FLOWTRAN to Model Solids-Handling Equipment," *Comput. Chem. Eng.*, **4**, 49 (1980).
Nienow, A. W., and R. Conti, "Particle Abrasion at High Solids Concentration in Stirred Vessels," *Chem. Eng. Sci.*, **33**, 1077 (1978).
Ouchiyama, N., and T. Tanaka, "Porosity Estimation for Random Packings of Spherical Particles," *Ind. Eng. Chem. Fundam.*, **23**, 490 (1984).
Rajagopal, S., K. M. Ng, and J. M. Douglas, "Design of Solids Processes: Production of Potash," *Ind. Eng. Chem. Res.*, **27**, 2071 (1988).
Rajagopal, S., K. M. Ng, and J. M. Douglas, "A Hierarchical Procedure for the Conceptual Design of Solids Processes," *Comput. Chem. Eng.*, **16**, 675 (1992).
Ramabhadran, T. E., and J. H. Seinfeld, "Self-Preserving Theory of Particulate Systems," *Chem. Eng. Sci.*, **30**, 1019 (1975).
Ramabhadran, T. E., T. W. Peterson, and J. H. Seinfeld, "Dynamics of Aerosol Coagulation and Condensation," *AIChE J.*, **22**, 840 (1976).
Ramkrishna, D., "Solution of Population Balance Equations," *Chem. Eng. Sci.*, **26**, 1134 (1971).
Rossiter, A. P., and J. M. Douglas, "Design and Optimisation of Solids Processes: 1. A Hierarchical Decision Procedure for Process Synthesis of Solids Systems," *Chem. Eng. Res. Des.*, **64**, 175 (1986a).
Rossiter, A. P., and J. M. Douglas, "Design and Optimisation of Solids Processes: 2. Optimization of Crystalliser, Centrifuge and Dryer Systems," *Chem. Eng. Res. Des.*, **64**, 184 (1986b).
Saleeby, E. G., and H. W. Lee, "Solution and Analysis for Crystallization with Agglomeration," *Chem. Eng. Sci.*, **49**, 1879 (1994).
Sastry, K. V. S., and P. Gaschignard, "Discretization Procedure for the Coalescence Equation of Particulate Processes," *Ind. Eng. Chem. Fund.*, **20**, 355 (1981).
Shah, B. H., D. Ramkrishna, and J. D. Borwanker, "Simulation of Particulate Systems Using the Concept of the Interval of Quiescence," *AIChE J.*, **23**, 897 (1977).
Shook, C. A., D. B. Haas, W. J. W. Husband, and M. Small, "Breakage Rates of Lignite Particles During Hydraulic Transport," *Can. J. Chem. Eng.*, **56**, 448 (1978).
Stinson, S. C., "Chiral Drugs," *Chem. Eng. News*, **72**, 38 (1994).
Synowiec, P., A. G. Jones, and P. A. Shamlou, "Crystal Break-up in Dilute Turbulently Agitated Suspensions," *Chem. Eng. Sci.*, **48**, 3485 (1993).
Ziff, R. M., "An Explicit Solution to a Discrete Fragmentation Model," *J. Phys. A: Math. Gen.*, **25**, 2569 (1992).

Manuscript received June 17, 1996, and revision received Sept. 19, 1996.